Raman Laser Spectrometer: Application to 12C/13C Isotope Identification in CH4 and CO2 Greenhouse Gases

Vladimir Vitkin, Anton Polishchuk, Ian Chubchenko, Evgeniy Popov, Konstantin Grigorenko, Artem Kharitonov, Arsen Davtian, Anton Kovalev, Valeria Kurikova, Patrice Camy, et al.

applied sciences

MDPI

Article

Raman laser spectrometer: Application to $^{12}C/^{13}C$ isotope identification in CH_4 and CO_2 greenhouse gases

Vladimir Vitkin [1], Anton Polishchuk [1], Ian Chubchenko [1], Evgeniy Popov [1], Konstantin Grigorenko [1], Artem Kharitonov [1], Arsen Davtian [1], Anton Kovalev [1], Valeria Kurikova [1], Patrice Camy [2], Pavel Loiko [2], Magdalena Aguiló [3], Francesc Díaz [3] and Xavier Mateos [3,*]

[1] ITMO University, 49 Kronverksky Pr., 197101 St. Petersburg, Russia; e-mail: v.v.v@bk.ru
[2] Centre de Recherche sur les Ions, les Matériaux et la Photonique (CIMAP), UMR 6252 CEA-CNRS-ENSICAEN, Université de Caen, 6 Boulevard du Maréchal Juin, 14050 Caen, France
[3] Universitat Rovira i Virgili (URV), Física i Cristal·lografia de Materials i Nanomaterials (FiCMA-FiCNA)-EMaS, Marcel.li Domingo 1, 43007 Tarragona, Spain
* Correspondence: xavier.mateos@urv.cat

Received: date; Accepted: date; Published: date

Featured Application: The developed Raman laser gas spectrometer is suitable for detection of carbon isotopologues of methane and carbon dioxide in human exhalation.

Abstract: A compact Raman laser gas spectrometer is developed. It comprises a high-power green laser at 532.123 nm as an excitation source and a specially designed gas cell with an internal volume less than 0.6 cm^3 withstanding gas pressures up to 100 atm. The resolution of the spectrometer is ~1 cm^{-1}. The Raman spectra of chemically pure isotopically enriched carbon dioxide ($^{12}CO_2$, $^{13}CO_2$) and methane ($^{12}CH_4$, $^{13}CH_4$) gases are studied. The expected limit of detection (LOD) is less than 100 ppm for the isotopologues of CO_2 and less than 25 ppm for those of CH_4 (at a gas pressure of 50 atm.), making the developed spectrometer promising for studying the sources of emissions of greenhouse gases by resolving their isotopologue composition. We also show the suitability of the spectrometer for Raman spectroscopy of human exhalation.

Keywords: Raman laser spectrometer; carbon isotopes; greenhouse gases; carbon dioxide; methane; human exhalation.

1. Introduction

Nowadays, the concentration of greenhouse gases (such as CO_2, CH_4, N_2O, etc.) in the atmosphere is increasing due to the anthropogenic emissions. Thus, there is a need to determine the anthropogenic contribution against the natural background and to recognize emissions from various industries [1-3]. One possibility for doing this is via the carbon isotope (^{12}C and ^{13}C) ratio measurements of carbon dioxide (CO_2) and methane (CH_4) in the atmospheric air [4,5].

So far, the isotope ratio Raman spectroscopy of CO_2 was addressed in several research works. In [6], the authors have found a way for determining the isotope-delta values (the relative difference of isotope ratios with respect to the reference material) $\delta^{13}C$ using micro-Raman spectroscopy. A technique for monitoring $^{13}CO_2$ by cavity-enhanced Raman spectroscopy was developed in [7]. Quantitative analysis of carbon isotopic composition in CO_2 with the estimation of the measurement uncertainty was performed in [8]. A detailed experimental and theoretical study on isotopic surface-enhanced Raman Spectroscopy was done in [9].

Defining the isotopic composition of greenhouse gases helps to constrain global budgets and to study sink and source processes [10]. CH_4 is an important anthropogenic and natural greenhouse gas and, moreover, it participates in atmospheric chemistry through its reaction with the hydroxyl radical [11]. Since individual CH_4 sources have characteristic isotope signatures, carbon and hydrogen isotope ratios of CH_4 (e.g., $\delta^{13}C$ - CH_4) have been useful to constrain the global methane budget [12].

By precisely measuring the ratio of ^{13}C to ^{12}C, one is able to determine the source of methane [13]. The individual values depend on the mechanisms of the CH_4 formation and consumption prior to its release to the atmosphere. It was shown [14] that it is possible to accurately measure the methane content in natural gases using Raman spectroscopy. The results of this work show the possibility of isotope-ratio analysis of methane.

Nowadays, isotope ratio measurement systems based on optical spectrometers are used because of several advantages. The first one is the fundamental possibility to distinguish the isotopologues (molecules that differ only in their isotope composition) with the same molecular weight but different isotopic composition like $^{16}O^{13}C^{16}O$ and $^{16}O^{12}C^{17}O$ (both representing carbon dioxide) [15]. Second, it is possible to perform calibration-free absolute measurement of isotopologues based on *ab initio* calculations of line intensities [16]. This is a relevant possibility in the metrology of isotope ratios because the International Committee for Weights and Measures (CIPM) encourages the development of absolute isotope ratio measurement values for reference materials [17]. Third, such systems are relatively easy in use, field deployable and low cost. They require no complicated sample preparation, provide real-time data, and allow for *in situ* monitoring with a spectroscopic selectivity. The disadvantage of the isotope ratio optical spectrometers compared to mass spectrometers is still low accuracy [18].

Raman spectroscopy has advantages over traditional methods in the analysis of pure isotopologues. Due to different selection rules, Raman spectroscopy can detect even diatomic homonuclear molecules such as O_2 or N_2 [19-22]. The development of Raman-based gas analyzers was presented in several papers [23,24]. A system for analysis of mixtures of CO and H_2 (synthesis gas) was proposed in [25]. The Purcell enhanced Raman scattering (PERS) device was used for isotopic gas analysis in [26]. A Raman analyzer for sensitive natural gas composition analysis was described in [27]. The main limitation is the low intensity of Raman scattering from gases. So far, application of Raman spectroscopy for routine trace gas analysis have not found widespread use due to the inherent weakness of Raman transitions and it was mainly employed in condensed phases [28]. The above mentioned limitation can be overcome by using intense excitation beams and high-pressure gas cavities. For the reliable $^{13}C/^{12}C$ ratio measurements, it is critical to calibrate the instruments. The preparation of calibration gas mixtures requires the analysis of the parent gases, such as pure $^{12}CO_2$ and $^{13}CO_2$ [29].

In the present work, we report on the method of quantitative analysis of $^{12}CO_2$, $^{13}CO_2$, $^{12}CH_4$ and $^{13}CH_4$ greenhouse gases based on Raman laser gas spectroscopy.

2. Materials and Methods

This study is dedicated to the development of a compact Raman laser gas spectrometer suitable for the analysis of gases under high pressures. The details of the spectrometer are described in Section 3.

The isotopically enriched carbon dioxide ($^{12}CO_2$, $^{13}CO_2$) and methane ($^{12}CH_4$ and $^{13}CH_4$) gases were studied. The CO_2 gases were provided by PA EXP, Ltd. (Russia) and the CH_4 ones – by the Cambridge Isotope Laboratories (USA). The chemical purity (CP) and carbon isotopic enrichment (δC) of the studied gases are specified in Table 1 (provided by the suppliers). The chemical purity shows the molar content of the main gas component and equals to 100% minus the total content of impurities (e.g., N_2, O_2, Ar, CO, etc.). It is measured by gas chromatography–mass spectrometry (GC-MS). The carbon isotopic enrichment shows the content of the target isotopologue in the main gas component and it is measured by isotope-ratio mass spectrometry (IRMS). The gas temperature was 293 K.

Table 1. Chemical purity (CP) and Carbon isotopic enrichment (δC) of the studied carbon dioxide and methane gases.

Gas	CP, %	δC, %
$^{12}CO_2$	>99.987	99.992
$^{13}CO_2$	>99.994	99.57
$^{12}CH_4$	>99.5	>99.99
$^{13}CH_4$	>99	>99.9

This work also includes the study of human exhalation. All subjects gave their informed consent for inclusion before they participated in the study. The study was conducted in accordance with the Declaration of Helsinki, and the protocol was approved by the Ethics Committee of ITMO University (project RFMEFI57518X0180).

3. Raman laser spectrometer

3.1. Excitation source

The scheme of the spectrometer is shown in Fig. 1. As the excitation source, we employed a continuous-wave diode-pumped solid-state laser (MSL-R-532, CNI-Lasers) emitting ~5 W of linearly polarized output at a wavelength of 532.123 nm with a full-angle divergence of 1.5 mrad, the beam quality parameter $M^2_{x,y} < 1.1$ (TEM_{00} mode) and a laser linewidth of <1 pm (~0.03 cm^{-1}). The excitation beam was expanded using a ×7 Vega laser beam expander (λ = 532 nm, Edmund Optics) and focused into the gas cell using a specially designed doublet lens with a focal length f = 55.9 mm with both sides antireflection (AR) coated at 532 nm. The measured spot size in the focus was less than 10 μm (diameter, as measured by the optical knife method). The peak on-axis laser intensity was then about ~10 MW/cm^2. More details about the focusing system can be found elsewhere [30].

Prior to the beam expanding system, we installed a system based on a pair of crossed polarizers (P1 and P2) and a $\lambda/2$ waveplate and a Faraday rotator placed between them. It prevented back-scattered light from damaging the excitation laser. In addition, a pair of flat highly-reflective (HR) mirrors was used to align precisely the focal spot position in the gas cell, Fig. 1(b).

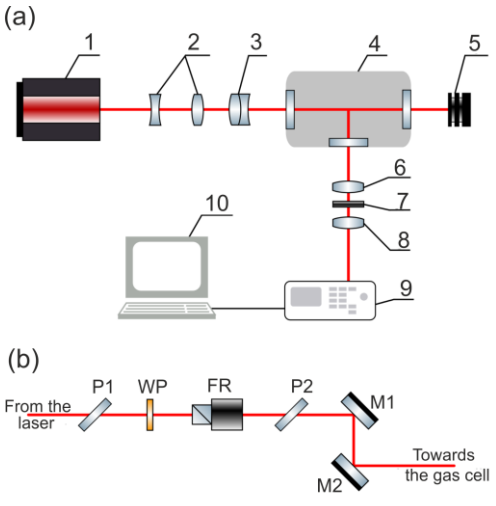

Figure 1. (a) Scheme of the Raman gas spectrometer: 1 – excitation laser, 2 – lens expander, 3 – focusing lens, 4 – gas cell, 5 – laser radiation absorber, 6 – collecting lens, 7 – notch filter, 8 – focusing lens, 9 - spectrometer, 10 – computer; (b) System for attenuation and optical alignment of the laser beam: P1 and P2 – polarizers, WP – half-wave plate, M1, M2 – HR mirrors.

3.2. High-pressure gas cell

A special gas cell made of titanium was developed, Fig. 2. It was designed to work with gases in a limited volume with high pressure. The internal volume was only 0.57 cm^3. To prevent reflections and light scattering, the internal surfaces of the gas cell were coated with an anti-glare enamel. The

two optical windows for the excitation and scattered beams were made of K8 optical glass. The detection was at 90° to the optical axis of the laser beam. The gas cell can withstand pressures up to ~100 atm. Note that CO_2 passes from the gaseous to liquid phase at a pressure of ~60 atm.

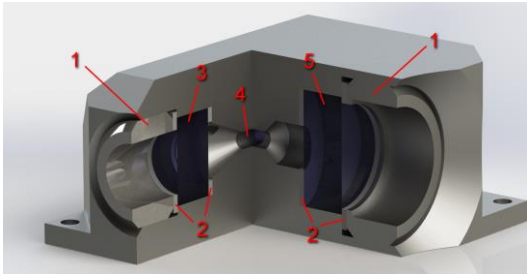

Figure 2. The scheme of the high-pressure gas cell: 1 – nut rings, 2 - PTFE gaskets, 3 – input window for passing the excitation light, 4 – useful volume for the studied gas, 5 – output window for collection of the scattered light.

The thickness of the optical windows was determined based on the calculations of the stress and displacement fields in the windows using the SolidWorks software, Fig. 3(a)-(d). The ultimate stress for both windows was assumed to be below the elastic limit of the K8 glass, ~40 MPa, Fig. 3(e). Under these conditions, the minimum thickness of the windows is 8 mm with a deviation from flatness of 2 μm when exposed to a pressure of 100 atm. We have selected the thickness of 8 mm for both windows. The clear aperture (diameter) of the windows was ~10 mm (for the excitation beam) and 15 mm (for the scattered light). The input window was AR coated for 532 nm and the output one – for 420-680 nm. The calculated fraction of the collected Raman signal determined by the geometry of the gas cell is 11%.

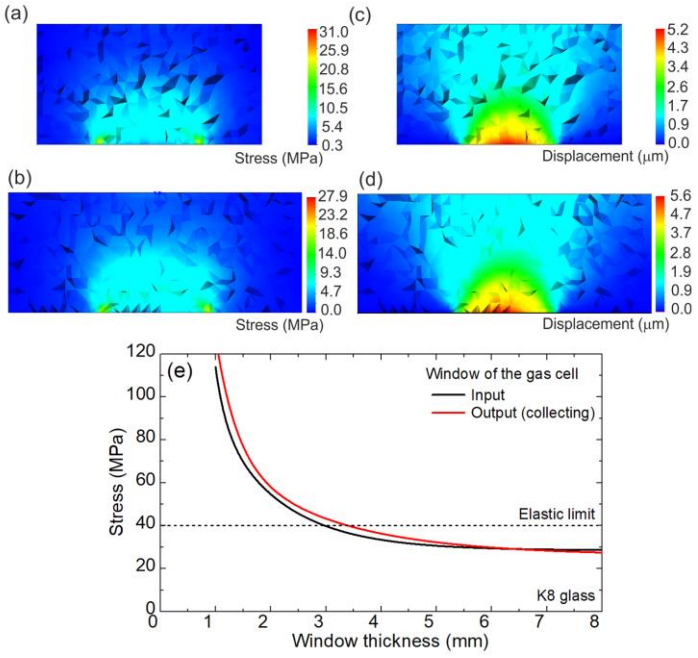

Figure 3. (a)-(d) Simulation of (a),(b) the stress field, σ, and (c),(d) the field of total displacements, u, in (a),(c) the input window of the gas cell and (b),(d) the output window used for collection of the scattered light. The gas pressure is 100 atm; (e) Calculated maximum stress in the window *vs*. its thickness, the dashed line represents the elastic limit of the K8 glass (the window material). The grain structure in (a)-(d) represents the mesh used in the simulations.

The gas cell was equipped with a gas inlet and an outlet. First, a backing vacuum pump was connected to the outlet valve and the cell was evacuated to the pressure of 10^{-3} mm Hg. Then, the

inlet valve was opened and the cell was filled in with the studied or reference gas. After the measurement, we released the gas into the evacuation system through the outlet valve.

3.3. Spectrometer

The scattered light was collected using an achromatic doublet lens (f = 55.9 mm) AR-coated for 420-680 nm. The Rayleigh scattered light was filtered out using a pair of notch filters (attenuation at 532 nm: $\times 10^{-12}$). Another achromatic doublet lens (f = 80.6 mm) was used to reimage the scattered light at the input slit of the spectrometer. It had the same AR coating as for the collecting lens.

The spectrometer was based on a Czerny-Turner scheme. A diffraction grating with 1800 grooves per mm with a blazing wavelength of 500 nm was used. Its spectral efficiency at 330-860 nm exceeded 40%. The linear dispersion of the system was 1.52 nm/mm and the spectral resolution (the instrumental linewidth, full width at half maximum (FWHM)) was 0.05 nm. The reproducibility of the wavelength setting was 0.03 nm. To find a compromise between the spectral resolution and the signal-to-noise (SNR) ratio, the width of the entrance slit was ~20 μm during the experiments. For detecting the spectra, we used a CMOS camera (Hamamatsu) with a 2048×122 pixel^2 grid (pixel size: 12×12 μm). It was cooled by a Peltier element to -40 °C. The exposure time varied from 10 μs up to 10 min. The projected spectral range was as long as 35 nm (0.017 nm per pixel). It was possible to shift this range within the interval 530-635 nm. More details can be found in [31].

The wavelength grading was performed using an Hg-He arc-discharge spectral lamp (DRGS-12). The calibration of the Raman spectrometer was performed using a certified reference material of toluene with a known Raman spectrum [32]. The determined relative standard deviation (Δ_{rel}) between the measured and standard peak Raman shifts of toluene was <0.01% for the range of Raman shifts of 1000-3300 cm^{-1} (for λ_{exc} = 532.123 nm). The spectral resolution of the spectrometer was ~1 cm^{-1} (the instrumental linewidth, FWHM). The measurements are performed at room temperature (293 K).

4. Spectroscopy of ^{12}C/^{13}C isotopologues

The study of greenhouse gas mixtures containing the gases of interest (i.e., carbon dioxide and methane) requires a preliminary study of the reference gases with high chemical and isotopic purity.

The Raman spectra of the carbon isotopologues of carbon dioxide and methane are known. Here, we briefly describe and interpret the measured spectra.

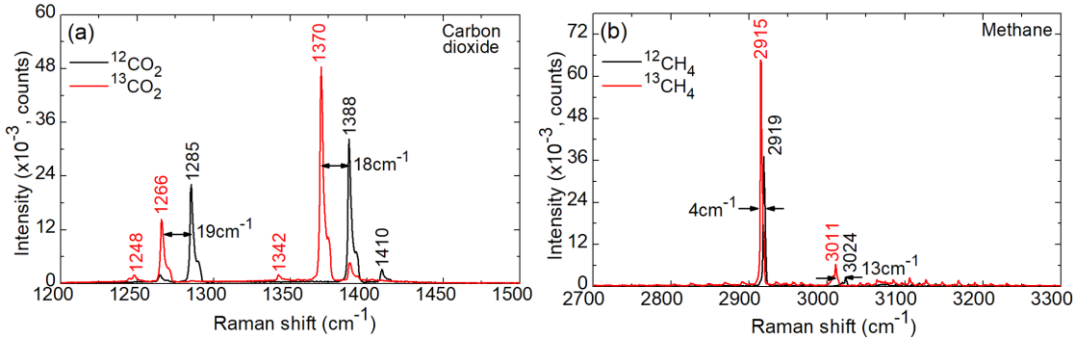

Figure 4. Raman spectra of isotopically enriched (a) carbon dioxide ($^{12}CO_2$ and $^{13}CO_2$) and (b) methane ($^{12}CH_4$ and $^{13}CH_4$) gases. The excitation wavelength λ_{exc} = 532.123 nm; the resolution is ~1 cm^{-1}. Gas pressure: 1 atm. Exposure time: 60 s.

The CO_2 molecule is linear and centrosymmetric. The Raman spectrum of CO_2, see Fig. 4(a), contains two intense and sharp Q-branches which form the diad ν_1 (1388 / 1370 cm^{-1}) and $2\nu_2$ (1285 / 1266 cm^{-1}) for the ^{12}C / ^{13}C containing molecules, respectively [33]. Adjacent to these lines, there are much weaker ones assigned as $\nu_1 + \nu_2 - \nu_2$ (1410 cm^{-1} for ^{12}C, for ^{13}C, it overlaps with the ν_1 line) and $3\nu_2 - \nu_2$ (1266 / 1248 cm^{-1} for ^{12}C / ^{13}C, respectively). The easiest attribution of the carbon isotopologues of CO_2 is according to the ν_1 and $2\nu_2$ diad: the wavenumber shift between the corresponding lines for

the $^{12}CO_2$ and $^{13}CO_2$ molecules is ~18-19 cm^{-1}. The Raman lines of isotopologues of carbon dioxide are easily detectable even at low gas pressure (1 atm.) using isotopically-enriched gases.

The Raman spectra of the $^{12}CH_4$ isotopologue have been systematically studied. Much less information is present about the second most abundant natural isotopologues, $^{13}CH_4$ [34]. Only recently, several studies focused on filling in this gap [35]. CH_4 has tetrahedral symmetry (point group T_d) with four normal modes of vibration. They are labeled by irreducible representations of the T_d point group. The fundamental frequencies exhibit a simple relation, $\nu_1(A_1) \approx \nu_3(F_2) \approx 2\nu_2(E) \approx 2\nu_4(F_2)$. It leads to the so-called polyad structure in the Raman and IR spectra [36]. A polyad P_n gathers all vibrational states (ν_1, ν_2, ν_3 and ν_4) satisfying the condition $n = 2(v_1 + v_3) + v_2 + v_4$, where v_i are the vibrational quantum numbers for i-th (i = 1, 2, 3, 4) mode. Each set of {v_i} defines a vibrational level. The pentad P_2 corresponds to 5 vibrational levels: $2\nu_4$, $\nu_2 + \nu_4$, $2\nu_2$, ν_1 and ν_3. The lines in the Raman spectra corresponding to the pentad of methane are observed at ~3000 cm^{-1} and they can be used for detection of isotopologues of CH_4.

The Raman spectra of isotopologues of methane around ~3000 cm^{-1} have a rich structure due to the complex vibration-rotation polyad interaction. The most intense line is observed at ~2919 cm^{-1} ($^{12}CH_4$) and 2915 cm^{-1} ($^{13}CH_4$) and is assigned as ν_1. The isotope wavenumber shift is only ~4 cm^{-1}. This line is well detected even at low gas pressure and short exposure, Fig. 4(b). Other prominent lines are those at ~3024 cm^{-1} ($^{12}CH_4$) and 3011 cm^{-1} ($^{13}CH_4$) showing higher isotope wavenumber shift whilst much lower intensity.

The spectra from Fig. 4 were analyzed to determine the limit of detection (LOD) for each of the gases, Table 2. First, the Raman intensity at the characteristic Raman shift (ν) was determined both for the signal (I_{signal}) and noise (I_{noise}) yielding the useful signal, $\Delta I_{signal} = I_{signal} - I_{noise}$. The room mean square value of the noise, $(r.m.s.)_{noise}$, was also determined. The noise analysis was performed using the spectra of isotopically enriched gases in the wavenumber range free of Raman lines covering about ~1000 cm^{-1}. The LOD is:

$$\mathrm{LOD}_{\mathrm{vol\%}} = X_{\mathrm{vol\%}} \frac{3(r.m.s.)_{\mathrm{noise}}}{\Delta I_{\mathrm{signal}}}. \quad (1)$$

Here, $X_{vol\%}$ is the volume fraction of the studied gas which is close to 100% for chemically pure isotopically enriched gases, cf. Table 1. The results on LOD are shown in Table 2 being expressed both in vol% and parts per million (ppm), $LOD_{ppm} = 10^4 \times LOD_{vol\%}$.

The upper limit for the error in the LOD estimation was determined by analyzing 10 repetitive measurements for the $^{12}CH_4$ gas. The maximum deviation from the average LOD value was ~14%.

Table 2. Analysis[a] of the Sensitivity of the Raman Gas Spectrometer According to the Study of Chemically Pure Isotopically Enriched Carbon Dioxide and Methane Gases

Parameter	**$^{12}CO_2$**	**$^{13}CO_2$**	**$^{12}CH_4$**	**$^{13}CH_4$**
ν, cm^{-1}	1388	1370	2919	2915
I_{signal}, counts	7630	13754	37487	64654
I_{noise}, counts	382	229	523	311
$(r.m.s.)_{noise}$, counts	28	27	30	28
ΔI_{signal}, counts	7248	13525	36964	64343
LOD(1 atm.), %	1.1731	0.5952	0.2428	0.1303
LOD(50 atm.), %	*0.0227*	*0.0119*	*0.0049*	*0.0026*
LOD(50 atm.), ppm	*227*	*119*	*49*	*26*
LOD(50 atm., 300 s), ppm	*95*	*50*	*20*	*11*

[a]The Raman spectra are shown in Fig. 4, gas pressure: 1 atm., exposure time: 60 s. The estimated LOD values for the pressure of 50 atm. are according to Fig. 5. The error in the specified LOD values is 14%. The estimated values are given in *italics*.

The LOD can be decreased in two ways. One is the increase of the gas pressure. The limit of detection is proportional to inverse of the gas pressure p, LOD ~ 1/p, see Eq. (1). Indeed, the useful Raman signal of a gas in proportional to the gas pressure [37], while the noise level is mostly

determined by the detector and thus is independent on the pressure. To confirm this, we have measured the Raman spectra of chemically pure isotopically enriched $^{12}CO_2$ gas at various gas pressures in the range of 1 – 9 atm. keeping the same exposure time of 60 s. The resulting LOD values (according to the 1388 cm^{-1} Raman line) are shown in Fig. 5. The data agree well with the LOD ~ 1/*p* law, yielding an estimation of the limit of detection at the maximum available gas pressure (50 atm.) of 227 ppm (for 60 s exposure). Note that particularly for CO_2 at high pressures (>50 atm.), it was pointed out in [10] that the exponential law better describes the dependence of the Raman signal on the gas pressure. Further studies are thus required at such elevated pressures.

Using the data measured at 1 atm., we interpolated the dependences for other gases, as shown in Fig. 5 by dashed lines. The corresponding LOD(50 atm.) values are listed in Table 2. In particular, for methane, they are as low as 49 ppm ($^{12}CH_4$) and 26 ppm ($^{13}CH_4$).

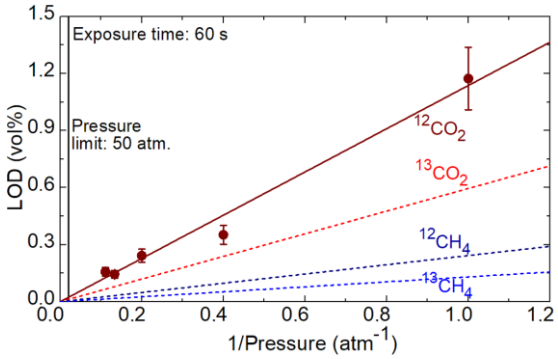

Figure 5. Limit of detection (LOD) of chemically pure isotopically enriched carbon dioxide and methane gases *vs*. inverse of the gas pressure: *symbols*: experimental data for $^{12}CO_2$ using the 1388 cm^{-1} Raman line, *solid line* – their linear fit, *dashed lines* – interpolation for other gases according to the measurement at 1 atm. Exposure time: 60 s.

Another possible way to improve the LOD is to increase the exposure time whilst this approach is of limited use for applications where relatively fast characterization is needed. As an example, we studied the $^{13}CH_4$ gas at a fixed pressure of 1 atm. and an exposure time Δt in the range of 1-60 s. The Raman spectra obtained for Δt = 1-30 s are presented in Fig. 6(a). Longer exposures allow observing weak spectral details of the $^{13}CH_4$ pentad.

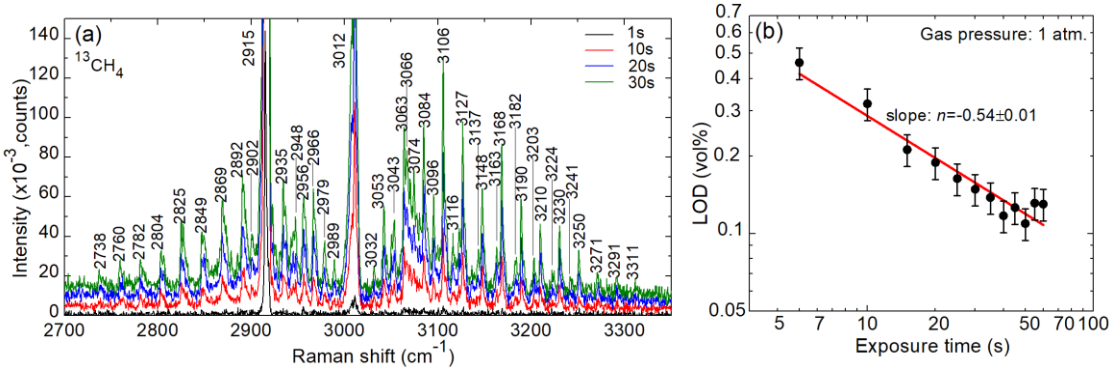

Figure 6. (a) Raman spectrum of high-purity (>99%) isotopically-enriched (>99.9% ^{13}C) $^{13}CH_4$ gas. The excitation wavelength λ_{exc} = 532.123 nm; the resolution is ~1 cm^{-1}. Gas pressure: 1 atm. Exposure time Δt: 1 – 30 s; (b) Double-logarithmic plot of LOD *vs*. the exposure time: *symbols*: experimental data, *line*: linear fit according to Eq. (2). Gas pressure: 1 atm.

The dependence of LOD on the exposure time Δt, plotted in a double-logarithmic scale, is shown in Fig. 6(b). From statistics, it is known that the r.m.s. of an average value is reduced by a factor of $N^{-0.5}$ with respect to that for a single measurement, where N is the number of measurements which are averaged. Thus, if Δt_0 = 1 s measurement yields a limit of detection of LOD_0, any longer

measurement with $\Delta t = s \times \Delta t$ can be represented as a set of s elementary measurements with $\mathrm{LOD}(\Delta t) = \mathrm{LOD}_0 \times s^{-0.5} = \mathrm{LOD}_0 \times (\Delta t/\Delta t_0)^{-0.5}$. By plotting Fig. 6(b) in double-logarithmic scale and fitting the experimental points by a linear function, we obtain the slope n of the dependence:

$$\mathrm{LOD}(\Delta t) = \mathrm{LOD}_0 \left(\frac{\Delta t}{\Delta t_0} \right)^{-n}. \quad (2)$$

In our case, n = -0.54±0.01 which agrees well with the theoretical considerations.

By considering both the effects of the increased gas pressure (p = 50 atm.) and the exposure time (Δt = 300 s), we obtained lower-limit estimations of LOD for all four studied gases, cf. Table 2, i.e., <100 ppm for the isotopologues of carbon dioxide and <25 ppm for those of methane.

5. Towards applications: Human exhalation

Raman spectroscopy is well suited for the simultaneous detection of various gases in the analysis of human respiration [38]. Natural carbon isotopes (^{12}C and ^{13}C) present in the human breath can be used to identify various diseases. Carbon isotopes in exhaled CO_2 can be a valuable real time biomarker of cachexia [39] (depletion of the body), associated with the acute phase of the reaction caused by endotoxemia (accumulation of toxic substances in the body). The acute phase reaction causes shifts in stable carbon isotopes in exhaled CO_2, which can be used to monitor nutrient metabolism. Isotope mass spectrometry (IRMS) exists to determine CO_2 carbon isotopes in human respiration [40]. This method has high accuracy, sensitivity and stability, but it is rather complex, expensive and requires large expenditures on equipment and staff training. There is a less expensive way to detect CO_2 isotopes using an isotope-selective non-dispersive infrared spectrometer (NDIRS) [41], but it is only suitable for simple breath tests where a small number of samples are required, for example, to detect diseases of the gastrointestinal tract and detect Helicobacter bacteria pylori [42]. This is due to a decrease in the correlation of repeated measurements with longer series of measurements.

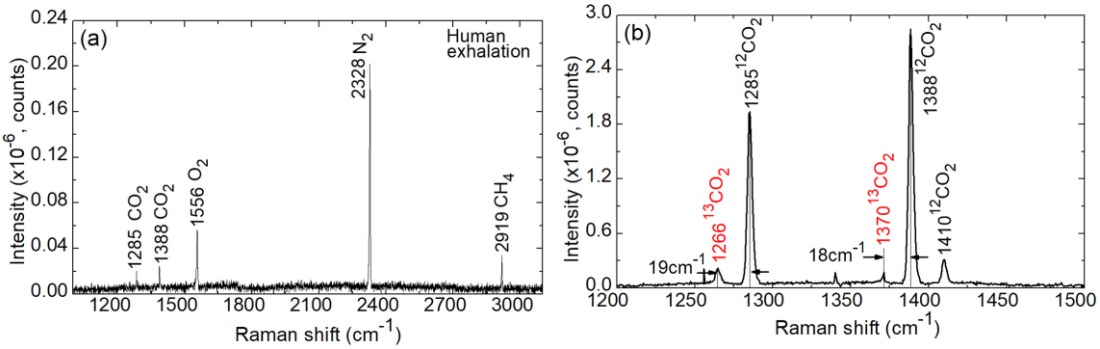

Figure 7. Raman spectrum of the human breath (exhalation): (a) an overview spectrum; (b) a close view on the $^{12}CO_2$ / $^{13}CO_2$ lines. The excitation wavelength λ_{exc} = 532.123 nm; the resolution is ~1 cm^{-1}. Gas pressure: 1 atm. Exposure time: (a) 30 s, (b) 600 s.

An overview Raman spectrum of a human exhalation measured at ambient pressure (1 atm.) is shown in Fig. 7(a). Its shows several intense Raman peaks at 1285 and 1388 cm^{-1} (both – $^{12}CO_2$), 1556 cm^{-1} (O_2), 2328 cm^{-1} (N_2) and 2919 cm^{-1} ($^{12}CH_4$). By focusing on the spectral range around ~1300 cm^{-1} and applying longer exposure (600 s), we were able to resolve clearly the Raman lines assigned to the isotopologues of carbon dioxide ($^{12}CO_2$ and $^{13}CO_2$). The spectral position of the lines and the isotopoc wavenumber shifts well agree with the data for isotopically enriched gases, cf. Fig. 4.

The Raman spectra of isotopologues of carbon dioxide were analyzed from the poit of view of LOD in order to confirm the values obtained with the isotopically enriched gases, see Fig. 4. Note that LOD can be calculated for any gas in a gas mixture if its volume fraction $X_{vol\%}$ is known, see Eq. (1). The volume fractions of $^{12}CO_2$ and $^{13}CO_2$ gases in the human exhalation depends on different factors, e.g., on the time between breathing in and out [43,44]. We will use the mean values of 4 vol%

290 $^{12}CO_2$ and 0.04 vol% $^{13}CO_2$. Based on these volume fractions and the measured Raman spectra,
291 Fig. 7(b), we have determined LOD to be 225 ppm ($^{12}CO_2$) and 75 ppm ($^{13}CO_2$) at a gas pressure of
292 1 atm. and an exposure time of 600 s. These values agree well with the analysis performed in Table 2
293 considering the difference in the exposure time.

294 **6. Conclusions**

295 To conclude, we have developed a sensitive and compact Raman laser spectrometer suitable for
296 analyzing gas mixtures containing such relevant greenhouse gases as carbon dioxide and methane.
297 In particular, it is capable of identifying the contributions of carbon isotopologues, such as $^{12}CO_2$ /
298 $^{13}CO_2$ and $^{12}CH_4$ / $^{13}CH_4$. The feature of the developed spectrometer is a specially designed gas cell
299 with the following advantages: (i) it can withstand high gas pressures (up to 100 atm.), (ii) it has a
300 relatively small internal volume of ~0.6 cm^3 relaxing the requirements for sample preparation, and
301 (iii) together with the optical scheme of the spectrometer, it ensures good collection efficiency for the
302 scattered light and, thus, low limits of detection (LODs) for the studied gases. By studying
303 isotopically-enriched $^{12}CO_2$ / $^{13}CO_2$ and $^{12}CH_4$ / $^{13}CH_4$ gases, we estimated easily accessible LODs of
304 less than 100 ppm for the isotopologues of carbon dioxide and less than 25 ppm for those of methane.
305 We also show the proof-of-the-concept of the suitability of the developed spectrometer for studying
306 the human exhalation.
307 Further work will focus on developing a gas analyzer using calibrated gas mixtures. Such Raman
308 gas spectrometer and gas analyzer are promising for studies of sources of pollution in the
309 atmosphere, combustion processes and human exhalation.
310 Potentially, the developed Raman gas spectrometer can be used for analyzing virus structures
311 in human exhalation.

312 **Author Contributions:**

313 Conceptualization and methodology, E.P., I.C., A.Kh., P.C. and P.L.; validation, A.P. and A.D.; formal analysis,
314 V.K.; investigation, V.V., I.C., E.P., A.P., A.D. and V.K.; data curation, A.K.; writing—original draft preparation,
315 I.C., K.G.; writing—review and editing, P.L., M.A. and F.D.; visualization, K.G. and V.K.; supervision, V.V.;
316 project administration, V.V. and X.M.; funding acquisition, V.V. All authors have read and agreed to the
317 published version of the manuscript.

318 **Funding:** This research was funded by Ministry of Education and Science of Russian Federation, grant number
319 RFMEFI57518X0180.

320 **Conflicts of Interest:** The authors declare no conflict of interest.

321 **References**

322 1. Rieker, G.B.; Giorgetta, F.R.; Swann, W.C.; Kofler, J.; Zolot, A.M.; Sinclair, L.C.; Baumann, E.; Cromer, C.;
323 Petron, G.; Sweeney, C.; Tans, P.P.; Coddington, I.; Newbury, N.R. Frequency-comb-based remote sensing
324 of greenhouse gases over kilometer air paths. *Optica* **2014**, *1*, pp. 290-298, doi: 10.1364/OPTICA.1.000290.
325 2. Ghosh, P.; Brand, W.A. Stable isotope ratio mass spectrometry in global climate change research. *Intern. J.*
326 *Mass Spectrom.* **2003**, *228*, pp. 1-33, doi: 10.1016/S1387-3806(03)00289-6.
327 3. Schneider, S.H. Detecting climatic change signals: are there any" fingerprints"?. *Science* **1994**, *263*, pp. 341-
328 347, doi: 10.1126/science.263.5145.341
329 4. Stevens, C.M.; Rust, F.E. The carbon isotopic composition of atmospheric methane. *J. Geophys. Res.: Oceans*
330 **1982**, *87*, pp. 4879-4882, doi: 10.1029/JC087iC07p04879.
331 5. Monteil, G.A.; Houweling, S.; Dlugockenky, E.J.; Maenhout, G.; Vaughn, B.H.; White, J.W.C.; Rockmann,
332 T. Interpreting methane variations in the past two decades using measurements of CH_4 mixing ratio and
333 isotopic composition. *Atmosph. Chem. Phys.* **2011**, *11*, pp. 9141-9153, doi: 10.5194/acp-11-9141-2011.
334 6. Li, J.J.; Li, R.X.; Dong, H.; Wang, Z.H.; Zhao, B.S.; Wang, N.; Cheng, J.H. Carbon isotopic compositions in
335 carbon dioxide measured by micro-laser Raman spectroscopy. *J. Appl. Spectr.* **2017**, *84*, pp. 237-241, doi:
336 10.1007/s10812-017-0457-8.
337 7. Keiner, R.; Frosch, T.; Massad, T.; Trumbore, S.; Popp, J. Enhanced Raman multigas sensing–a novel tool
338 for control and analysis of $^{13}CO_2$ labeling experiments in environmental research. *Analyst* **2014**, *139*, pp.
339 3879-3884, doi: 10.1039/C3AN01971C.

8. Li, J.; Li, R.; Zhao, B.; Guo, H.; Zhang, S.; Cheng, J.; Wu, X. Quantitative measurement of carbon isotopic composition in CO_2 gas reservoir by micro-laser Raman spectroscopy. *Spectrochim. Acta A Mol. Biomol. Spectrosc.* **2018**, *195*, pp. 191-198, doi: 10.1016/j.saa.2018.01.082.
9. Zhang, M.; Zhao, L.B.; Luo, W.L.; Pang, R.; Zong, C.; Zhou, J.Z.; Ren, B.; Tian, Z.Q.; Wu, D.Y. Experimental and theoretical study on isotopic surface-enhanced Raman spectroscopy for the surface catalytic coupling reaction on silver electrodes. *J. Phys. Chem. C* **2016**, *120*, pp. 11956-11965, doi: 10.1021/acs.jpcc.6b02252.
10. Prinzhofer, A.; Battani, A. Gas isotopes tracing: an important tool for hydrocarbons exploration. *Oil Gas Sci. Tehcnol.* **2003**, *58*, pp. 299-311, doi: 10.2516/ogst:2003018.
11. Naik, V.; Voulgarakis, A.; Fiore, A.M.; Horowitz, L.W.; Lamarque, J.F.; Lin, M.; Prather, M.J.; Young, P.J.; Bergmann, D.; Cameron-Smith, P.J.; et al. Preindustrial to present-day changes in tropospheric hydroxyl radical and methane lifetime from the Atmospheric Chemistry and Climate Model Intercomparison Project (ACCMIP). *Atmosph. Chem. Phys.* **2013**, *13*, pp. 5277-5298, doi: 10.5194/acp-13-5277-2013.
12. Bergamaschi, P.; Schupp, M.; Harris, G.W. High-precision direct measurements of $^{13}CH_4/^{12}CH_4$ and $^{12}CH_3D/^{12}CH_4$ ratios in atmospheric methane sources by means of a long-path tunable diode laser absorption spectrometer. *App. Opt.* **1994**, *33*, pp. 7704-7716, doi: 10.1364/AO.33.007704.
13. Bréas, O.; Guillou, C.; Reniero, F.; Wada, E. The global methane cycle: isotopes and mixing ratios, sources and sinks. *Isot. Environ. Health S.* **2001**, *37*, pp. 257-379, doi: 10.1080/10256010108033302.
14. Petrov, D.V.; Matrosov, I.I. Raman gas analyzer (RGA): Natural gas measurements. *Appl. Spectr.* **2016**, *70*, 1770-1776, doi: 10.1177/0003702816644611.
15. Prokhorov, I.; Kluge, T.; Janssen, C. A novel method of carbon dioxide clumped isotope analysis with tunable infra-red laser direct absorption spectroscopy. *EGUGA* **2016**, p. EPSC2016-3931, doi: 2016EGUGA..18.3931P.
16. Polyansky, O.L.; Bielska, K.; Ghysels, M.; Lodi, L.; Zobov, N.F.; Hodges, J.T.; Tennyson, J. High-accuracy CO_2 line intensities determined from theory and experiment. *Phys. Rev. Lett.* **2015**, *114*, p. 243001, doi: 10.1103/PhysRevLett.114.243001.
17. International Committee for Weights and Measures. Proceedings of Session I of the 104th meeting (9-10 March 2015). Available online: https://www.bipm.org/utils/en/pdf/CIPM/CIPM2015-I-EN.pdf (accessed on 29 August 2020).
18. van Geldern, R.; Nowak, M.E.; Zimmer, M.; Szizybalski, A.; Myrttinen, A.; Barth, J.A.; Jost, H.J. Field-based stable isotope analysis of carbon dioxide by mid-infrared laser spectroscopy for carbon capture and storage monitoring. *Anal. Chem.* **2014**, *86*, pp. 12191-12198, doi: 10.1021/ac5031732.
19. Siberio-Pérez, D.Y.; Wong-Foy, A.G.; Yaghi, O.M.; Matzger, A.J. Raman spectroscopic investigation of CH_4 and N_2 adsorption in metal–organic frameworks. *Chem. Mater.* **2007**, *19*, pp. 3681-3685, doi: 10.1021/cm070542g.
20. Keutel, D.; Seifert, F.; Oehme, K.L.; Asenbaum, A.; Musso, M. Evidence for negative cross correlations in vibrational dephasing in liquids: Isotropic Raman-line shift and width phenomena in isotopic mixtures of N_2 and O_2. *Phys. Rev. Lett.* **2000**, *85*, p. 3850, doi: 10.1103/PhysRevLett.85.3850.
21. Cabaço, M.I.; Longelin, S.; Danten, Y.; Besnard, M. Transient dimer formation in supercritical carbon dioxide as seen from Raman scattering. *J. Chem. Phys.* **2008**, *128*, p. 074507, doi: 10.1063/1.2833493.
22. Musso, M.; Matthai, F.; Keutel, D.; Oehme, K.L. Critical Raman line shape behavior of fluid nitrogen. *Pure Appl. Chem.* **2004**, *76*, pp. 147-155, doi: 10.1351/pac200476010147.
23. Yan, D.; Popp, J.; Frosch, T. Analysis of fiber-enhanced Raman gas sensing based on Raman chemical imaging. *Anal. Chem.* **2017**, *89*, pp. 12269-12275, doi: 10.1021/acs.analchem.7b03209.
24. Yu, A.; Zuo, D.; Wang, X. Optimization of parabolic cell for gas Raman analysis. *J. Raman Spectr.* **2019**, *50*, pp. 731-740, doi: 10.1002/jrs.5564.
25. Eichmann, S.C.; Weschta, M.; Kiefer, J.; Seeger, T.; Leipertz, A. Characterization of a fast gas analyzer based on Raman scattering for the analysis of synthesis gas. *Rev. Sci. Instrum.* **2010**, *81*, p. 125104, doi: 10.1063/1.3521397.
26. Petrak, B.; Cooper, J.; Konthasinghe, K.; Peiris, M.; Djeu, N.; Hopkins, A.J.; Muller, A. Isotopic gas analysis through Purcell cavity enhanced Raman scattering. *Appl. Phys. Lett.* **2016**, *108*, p. 091107, doi: 10.1063/1.4943146.
27. Sharma, R.; Poonacha, S.; Bekal, A.; Vartak, S.; Weling, A.; Tilak, V.; Mitra, C. Raman analyzer for sensitive natural gas composition analysis. *Opt. Eng.* **2016**, *55*, p. 104103, doi: 10.1117/1.OE.55.10.104103.

28. John, S.T.; Shaw, D.M.; Klug, D.D.; Patchkovskii, S.; Vankó, G.; Monaco, G.; Krisch, M. X-ray Raman spectroscopic study of water in the condensed phases. *Phys. Rev. Lett.* **2008**, *100*, p. 095502, doi: 10.1103/PhysRevLett.100.095502.
29. Chubchenko, Y.K.; Konopel'ko, L.A. Development of a new type of reference standard for carbon isotopic composition. *Measur. Tech.* **2018**, 60, pp. 1228-1232, doi: 10.1007/s11018-018-1344-2.
30. Vitkin, V.V.; Chubchenko, I.K.; Polischuk, A.V.; Kovalev, A.V.; Popov, E.E. Raman gas analyzer for detecting carbon isotopologues. *J. Physics: Conf. Ser.* **2019**, *1399*, p. 022033, doi: 10.1088/1742-6596/1399/2/022033.
31. Popov, E.; Polishchuk, A.; Grigorenko, K.; Chubchenko, I.; Vitkin, V. Raman detector of carbon isotopes. *Opt. Sens. and Det. VI* **2020**, *11354*, p. 113542P, doi: 10.1117/12.2556262
32. ASTM E1840-96, Standard Guide for Raman Shift Standards for Spectrometer Calibration; ASTM International: West Conshohocken, PA, USA, 1996.
33. Howard-Lock, H.E.; Stoicheff, B.P. Raman intensity measurements of the Fermi diad ν_1, $2\nu_2$ in $^{12}CO_2$ and $^{13}CO_2$. *J. Molec. Spectr.* **1971**, *37*, pp. 321-326, doi: 10.1016/0022-2852(71)90302-X.
34. Niederer, H.M.; Wang, X.G.; Carrington T., Jr.; Albert, S.; Bauerecker, S.; Boudon, V.; Quack, M. Analysis of the rovibrational spectrum of $^{13}CH_4$ in the Octad range. *J. Molec. Spectr* **2013**, *291*, pp. 33-47, doi: 10.1016/j.jms.2013.06.003.
35. Niederer, H.M.; Albert, S.; Bauerecker, S.; Boudon, V.; Champion, J.P.; Quack, M. Global analysis of the infrared spectrum of $^{13}CH_4$: lines in the region 0 to 3200 cm^{-1}. *CHIMIA Intern. J. Chem.* **2008**, *62*, pp. 273-276, doi: 10.2533/chimia.2008.273.
36. Boudon, V.; Rey, M.; Loete, M. The vibrational levels of methane obtained from analyses of high-resolution spectra. *J. Quant. Spectr. Rad. Transf.* **2006**, *98*, pp. 394-404, doi: 10.1016/j.jqsrt.2005.06.003.
37. Gooijer, C.; Ariese, F.; Hofstraat, J.W. *Chemical Analysis: A Series of Monographs on Analytical Chemistry and Its Application*; John Wiley & Sons: New York, NY, USA, 2000.
38. Okita, Y.; Katagiri, T.; Matsuura, Y. A Raman cell based on hollow optical fibers for breath analysis. In Optical Fibers and Sensors for Medical Diagnostics and Treatment Applications X, San Francisco, CA, USA, 24 February 2010; Publisher: International Society for Optics and Photonics, Vol. 7559, p. 755908, doi: 10.1117/12.841414.
39. Butz, D.E.; Cook, M.E.; Eghbalnia, H.R.; Assadi-Porter, F.; Porter, W.P. Changes in the natural abundance of $^{13}CO_2/^{12}CO_2$ in breath due to lipopolysacchride-induced acute phase response. *Rapid Commun. Mass Spectr.* **2009**, *23*, pp. 3729-3735, doi: 10.1002/rcm.4310.
40. Braden, B.; Haisch, M.; Duan, L.P.; Lembcke, B.; Caspary, W.F.; Hering, P. Clinically feasible stable isotope technique at a reasonable price: analysis of $^{13}CO_2/^{12}CO_2$-abundance in breath samples with a new isotope selective-nondispersive infrared spectrometer. *Z. Gastroenterol.* **1994**, *32*, pp. 675-678.
41. Barth, E.; Tugtekin, I.; Weidenbach, H.; Wachter, U.; Vogt, J.; Radermacher, P.; Adler, G.; Georgieff, M. Determination of $^{13}CO_2/^{12}CO_2$ ratio by IRMS and NDIRS. *Isot. Environ. Health S.* **1998**, *34*, pp. 209-213, doi: 10.1080/10256019708036348.
42. Koletzko, S.; Koletzko, B.; Haisch, M.; Hering, P.; Seeboth, I.; Hengels, K.; Braden, B. Isotope-selective non-dispersive infrared spectrometry for detection of Helicobacter pylori infection with ^{13}C-urea breath test. *The Lancet* **1995**, *345*, pp. 961-962, doi: 10.1016/S0140-6736(95)90704-1.
43. Normand, S.; Pachiaudi, C.; Khalfallah, Y.; Guilluy, R.; Mornex, R.; Riou, J. P. ^{13}C appearance in plasma glucose and breath CO_2 during feeding with naturally ^{13}C-enriched starchy food in normal humans. *Am. J. Clin. Nutr.* **1992**, *55*, pp. 430-435, doi: 10.1093/ajcn/55.2.430.
44. Schoeller, D.A.; Brown, C.; Nakamura, K.; Nakagawa, A.; Mazzeo, R.S.; Brooks, G.A.; Budinger, T. F. Influence of metabolic fuel on the $^{13}C/^{12}C$ ratio of breath CO_2. *Biomed. Mass Spectrom.* **1984**, *11*, pp. 557-561, doi: 10.1002/bms.1200111103.